Functionalized aerogels and aerogel inspired materials for different applications: photoactive molecules stabilization and accelerated release of drugs

N. Murillo-Cremaes[1], A. M. López[1], J. Saurina[2], A. Roig[1*], C. Domingo[1*]

[1]*Institut de Ciència de Materials de Barcelona (ICMAB-CSIC), Campus de la UAB, Bellaterra, Spain. E-mail: nmurillo@icmab.es*
[2]*Universidad de Barcelona, Dpt. Analytical Chemistry, Campus UB, Barcelona, Spain*

ABSTRACT

This study reports on the preparation of aerogel and aerogel-like nanoparticles and their impregnation, by following a procedure in supercritical carbon dioxide, with two different organic molecules with distinguished functionalities. Specifically, a photoactive molecule (triphenylpyrylium cation) was encapsulated in the restricted pores of silica aerogel and 300 nm silica nanoparticles, while a drug (triflusal and its metabolite, called HTB) was entrapped in silica aerogel and composite $Fe_3O_4@SiO_2$ nanoparticles. Excellent hybrid materials were obtained, improving the stability of the cation in water solutions and enhancing the bioavailability of the therapeutic agent.

INTRODUCTION

Aerogel and aerogel-inspired nanostructured materials are receiving considerable attention due to their broad variety of applications. Silica aerogels have been used in such different fields as construction or nanomedicine. It is well known that these systems are provided with a large intrinsic and accessible porosity. Typically, pore sizes range from less than 2 nm up to 300 nm. The properties of aerogels can be further enlarged and their applications broaden after being functionalized with another substance. In order to ensure a suitable environment for hosting, silicon oxide hosts have to meet some requirements: high specific surface areas allowing molecules accommodation and appropriate chemical groups to react with in case a stabilization of the guest substance is desired. One of the most interesting features of these hybrid compounds is the possibility to tune the release profile of the guest molecule depending on the nature of host-guest chemical interactions. The same matrix can promote the stabilization of unstable molecules or, on the contrary, make the discharge of the molecules that it is carrying easier.

The work we are presenting here focuses on the preparation, characterization and comparative analysis of several hybrid nanostructured materials based on silica matrices and organic guest molecules. Three silica-based porous matrices have been evaluated namely silica aerogel, [1] silica nanoparticles [2] and composite $Fe_3O_4@SiO_2$ nanoparticles. [3] The impregnation of these matrices with two different organic molecules was carried out by their dissolution in supercritical carbon dioxide. In particular, we will report on the utilization of aerogels and aerogel inspired materials as perfect systems to stabilize photoactive cations [4,
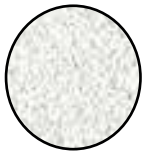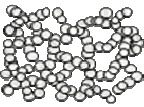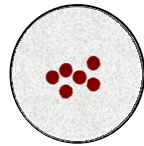
5] or to carry and enhance the bioavailability of a therapeutic agent. [6] To quantitatively monitor the release profile UV-Vis control and HPLC analysis were performed.

MATERIALS AND METHODS

Materials

The syntheses of the used matrices are fully described elsewhere. [1-3] The prepared materials (Table 1) consist in: i) transparent (aerogel monoliths) cylinders (AM samples) of about 0.8 x 2.4 cm and a density of 0.1 Kgm^{-3}, (ii) white, spongy and homogeneous aerogel-like powder (AP samples) composed of monodispersed spherical nanoparticles of ~ 300 nm diameter and 9 % polydispersity, and (iii) 65 nm composite $Fe_3O_4@SiO_2$ magnetic particles with 19 % polidispersity(CP samples).

Table 1. Schematic representation of the prepared matrices, synthetic method, specific surface area calculated by N_2 adsorption/desorption isotherms and encapsulated molecules by $scCO_2$ in each case.

Sample identification	Sketch	Preparation method	S_a (m^2/g)	Impregnated organic molecule	Impregnated sample identification
SiO_2 Aerogel-like NPs (AP)		Simultaneous sol gel and supercritical acetone drying	204.9	Pyrylium	Py@AP
SiO_2 Aerogel monoliths (AM)		Sol-gel and later supercritical methanol drying	433.4	Pyrylium Triflusal	Py@AM TRF@AM
$Fe_3O_4@SiO_2$ composite NPs (CP)		Simultaneous sol-gel and supercritical acetone drying	160.0	Triflusal	TRF@CP

The photoactive molecule chosen to be stabilized in the matrices was the organic cation 2,4,6- triphenylpyrylium (Ph_3Py^+, Py^+). [7, 8] The precursor used for its impregnation was the diketone 1,3,5-triphenyl-2-pentene-1,5-dione. Commercially available 2,4,6-triphenylpyryl tetrafluoroborate (Ph_3PyBF_4, $c-Py^+$) was purchased by Aldrich and used as reference for comparisons with encapsulated products. The drug used for impregnation was 2-acetyloxy-4-(trifluoromethyl) benzoic acid (TRF, triflusal). Moreover, the metabolite of triflusal (4-(trifluoromethyl) salicylic acid, HTB) was also analyzed. [9] TRF and its metabolite HTB were kindly donated by Uriach S.A., Spain. Carbon dioxide (99.995%) was supplied by Carburos Metálicos (Spain).

Equipment and procedure

Before impregnation and to ensure the total activation of the specific surface area in the host matrices, all of them were first calcinated at 300ºC during 2 h in a tubular oven under a N_2 atmosphere. Subsequently, the matrices were enclosed in cartridges made of 0.45 mm pore size paper, thus avoiding direct contact with the solutes. Pressurization and

depressurization cycles were carried out avoiding the formation of liquid CO_2 in the autoclave, which could damage the fragile porous structure of the aerogels and aerogel like-particles.

scCO$_2$ impregnation of Ph$_3$Py$^+$: Supercritical impregnation of pyryl cation was performed in batch mode in a high pressure equipment described elsewhere. [5, 10] Typically, liquified CO_2 was compressed by a syringe pump and delivered to a 0.1 L autoclave equipped with a vertical magnetic stirrer. The reactor was first charged with *ca.* 0.5 g of the matrix in the form of either AM or AP, and the precursor of the guest material (diketone) in a proportion of 20 wt%. The approach followed assumes that the cation synthesis proceeds in two steps: (i) diffusion at 150 bar and 60 ºC, followed by (ii) condensation at 130–150 ºC, performed separately in time. During the process, the autoclave was stirred at 400 rpm.

scCO$_2$ impregnation of TRF: Experiments to encapsulate the drug were carried out in a high pressure equipment running in the batch mode detailed previously. [11, 12] In a typical experiment, *ca.* 0.2 g of the matrix of either AM or CP were placed in a 100 mL reactor (TharDesing), whom contained triflusal in a proportion of 50 wt%. The autoclave was heated up to 45ºC and then pressurized with CO_2 at 200 bar. The system was stirred at 350 rpm and these conditions were kept during 5 h and 30 min.

Characterization

To make the morphological and structural characterization of the synthesized matrices, micrographs were obtained with a transmission electron microscopy (TEM) JEOL JEM-1210 operating at 120 kV. The BET specific surface area (S_a) was determined by N_2 adsorption–desorption measurements at 77 K using an ASAP 2000 Micromeritics Inc. instrument. Prior to measurements, samples were dried under a reduced pressure. The conditions used were 300 ºC over 24 h for aerogel particles and 100 ºC over 24 h for aerogel monoliths. To confirm the presence of the impregnated agent in the treated materials, Fourier transformed infrared (FTIR) spectra of the solid samples mixed with KBr were recorded on a Perkin-Elmer Spectrum One instrument. Materials impregnated with the therapeutic agent were analyzed by X-Ray diffraction and microdiffraction (XRD, Siemens D5000 X-ray powder difractometer, Microdiffratometer type) to confirm the desirable abscense of drug crystals as well as the crystallinity of magnetite nanoparticles in CP samples. Thermogravimetric analysis (TGA) of the modified silicas was performed in Ar using a TGA PerkinElmer 7 and a heating rate of 10 ºCmin^{-1} to evaluate loading efficiencies.

The matrices impregnated with the photoactive molecule were immersed in distilled water (pH = 6.5) for 12 days and exposed to natural light to evaluate their leaching behavior by UV-Vis spectroscopy (Cary 5 Varian UV/vis/NIR spectrophotometer).
The delivery profiles of matrices impregnated with triflusal were characterized in water using 0.01M HCl (pH 2) and 0.01M HCO_3^-/CO_3^{2-} (pH 7.4) solutions, which simulated the stomach and blood plasma pHs respectively, and using high liquid pressure chromatography (HPLC). Stirring rate and temperature were fixed at 70 rpm and 37ºC, respectively. The kinetic process was monitored following a reported procedure. [11]

RESULTS

Morphological characterization

Transmission electron microscopy images of raw matrices are presented in Fig. 1 (a, b, c). All the synthesized nanoparticles (NPs) were spherical in shape and possessed narrow size distributions. Photographs at macroscopic scale also appear in Fig. 1(e-h) Fig. 1(e, f) shows magnetic samples readily following a magnet (see Fig. 1e, f).
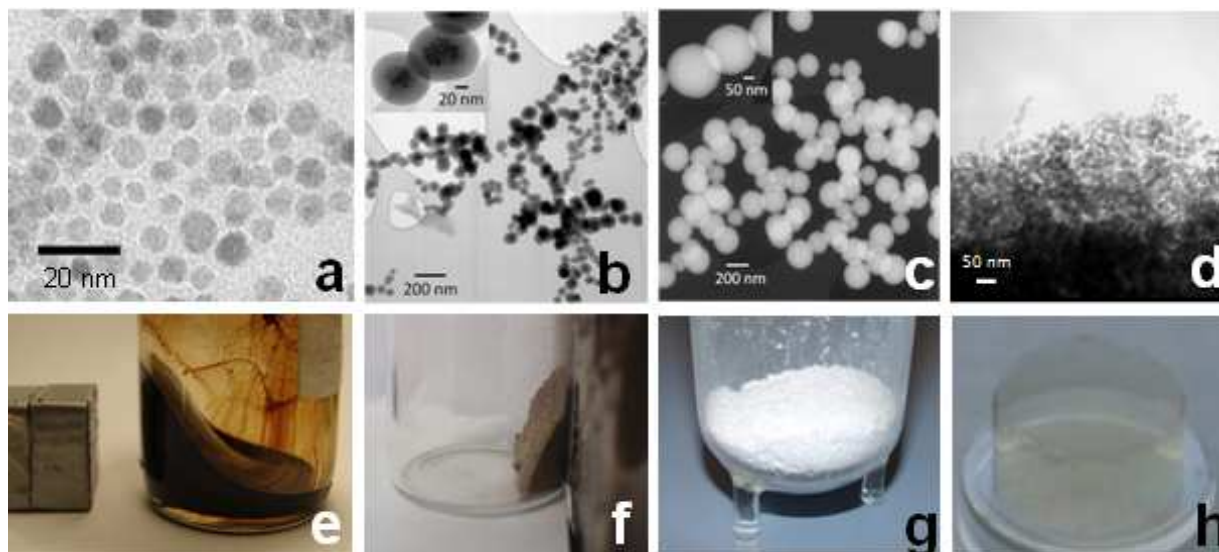
Figure 1. TEM images of a) magnetite NPs, b) Fe_3O_4@SiO_2 composite NPs (CP), c) SiO_2 NPs (AP), and d) SiO_2 aerogel monolith (AM) and their respective optical photographs: e) magnetite colloidal dispersion with a magnet, f) CP dry powder with a magnet, g) AP dry powder and h) AM block.

After impregnation with the photoactive molecule, the coloration of the resulting host materials was used as a first visual indication of the degree of success in the reaction (Fig. 2). The precursor of the guest molecule (diketone) was colorless, and only after cation formation a color appeared associated with absorption in the visible range. While the matrix was initially either transparent (AM in Fig. 2a) or white (AP in Fig. 2c), the adsorption of the organic cation was noticeably visible from the resulting yellow/orange color of the formed product (Fig. 2b, d). The uniform color of the pyrylium impregnated AM material is appreciated (sample Py$^+$@AM in Fig. 2b), indicating that diffusion of the precursor was homogeneous throughout the sample.

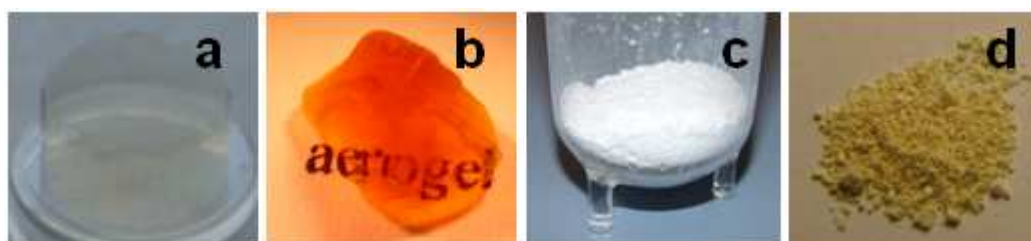**Figure 2.** Optical photographs of: a) pristine monolithic aerogel (AM) and b) impregnated sample Py$^+$@AM; c) pristine aerogel particles (AP) and d) impregnated sample Py$^+$@AP.

FTIR spectroscopy

In FTIR spectroscopy, absorption bands of Ph_3PyBF_4 appear between 1550 and 1650 cm^{-1} (a pick at 1625 cm^{-1} and a shoulder at 1600 cm^{-1}). [13, 14] The results obtained for the encapsulated products matched these characteristics peaks (Fig. 3a), demonstrating a successful formation of the pyryl cation during the supercritical impregnation process. The lack of C=O vibration bands at 1680–1650 cm^{-1}, typical from the diketone precursor, indicates moreover a high degree of transformation.
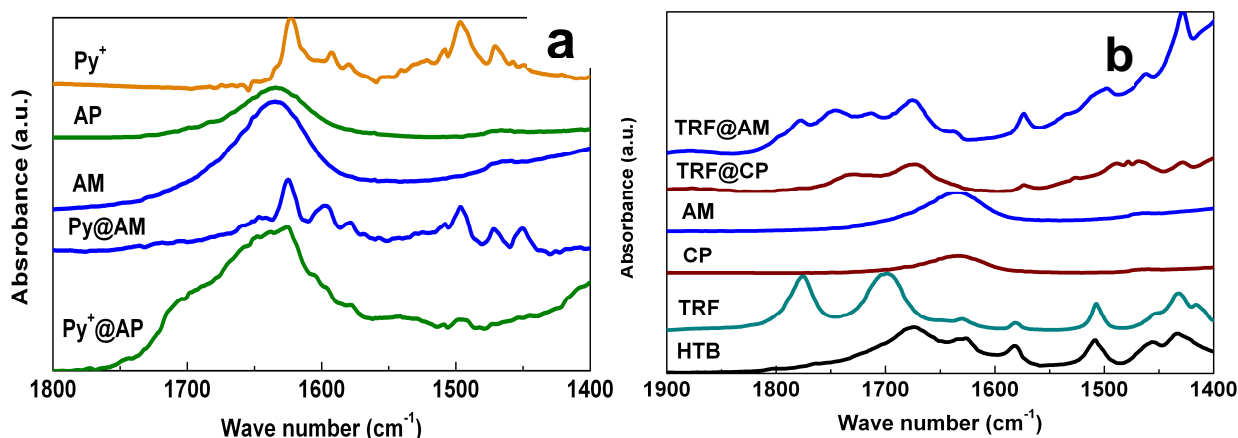
Figure 3. FTIR spectra of a) pristine matrices, commercial Ph_3PyBF_4 and impregnated matrices with pyrylium, and b) pristine matrices, commercials TRF and HTB and impregnated matrices with TRF.

Absorption peak found at 1770 cm^{-1} (Fig. 3b) is assumed as the most characteristic band of Triflusal, that corresponds to C=O stretching [12]. In the sample TRF@AM, the presence of the drug was demonstrated by this signal. FTIR bands at 1630, 1580 and 1505 cm^{-1} come also from TRF and HTB spectra. The first one cannot be used to identify the impregnated materials because it overlaps with the band of the absorbed water (see pristine matrices in Fig. 3b), the others bands were in both TRF@AM and TRF@CP samples. This indicates a proper encapsulation of the drug. The fact that peak considered as specifically TRF did not appear for impregnated composite NPs, may indicate that the drug was decomposed to HTB, an active hydrated metabolite of the TRF, due to a larger amount of water present in the untreated particles in comparison with the aerogel monolith.

Thermo gravimetric analysis

Thermogravimetric profiles of the pristine matrices and commercial guest molecules are shown in Fig. 4a and b, respectively. Particulate systems had an initial weight loss of ~ 2-7 wt% at temperatures lower than 150 °C, corresponding to the evaporation of adsorbed water (Fig. 4a). In the monolithic aerogel curve, however, there was no decay in this temperature range, which confirms that nanoparticles accommodate more water than monolith. In the temperature range 150–400 °C, the weight loss of untreated AM was insignificant, while for silica aerogel-like and composite NPs, although minor, it was measurable (*ca.* 0.5–1 wt%). Aerogel matrices also loss weight at temperatures higher than 450–500 °C because of material densification, and the reaction between silanol groups and the associated loss of water.

Commercial Ph_3PyBF_4 shows a decomposition profile characterized by an abrupt weight loss between 240 and 325 °C with its maximum slope at 300 °C, while triflusal decomposes in two steps, from 150 to 250 °C (loosing ~ 55 wt%) and in the temperature range of 250 and 360 °C, where the rest of the compound disintegrates (Fig. 4b).

AP matrix impregnated with the pyryl cation loosed water at temperatures lower than 180 °C, while the mass decay at temperatures higher than 200 °C was associated with the loss of the encapsulated Ph_3Py^+ (see Fig. 4c). When the cation is entrapped in the aerogel (AM), its decomposition occurs between 250 and 400 °C (maximum slope at 350 °C), as can be seen in Fig. 4c. This result indicates that the Ph_3Py^+ cation inside the nanopores presented a higher thermal stability than in the Ph_3PyBF_4 salt.
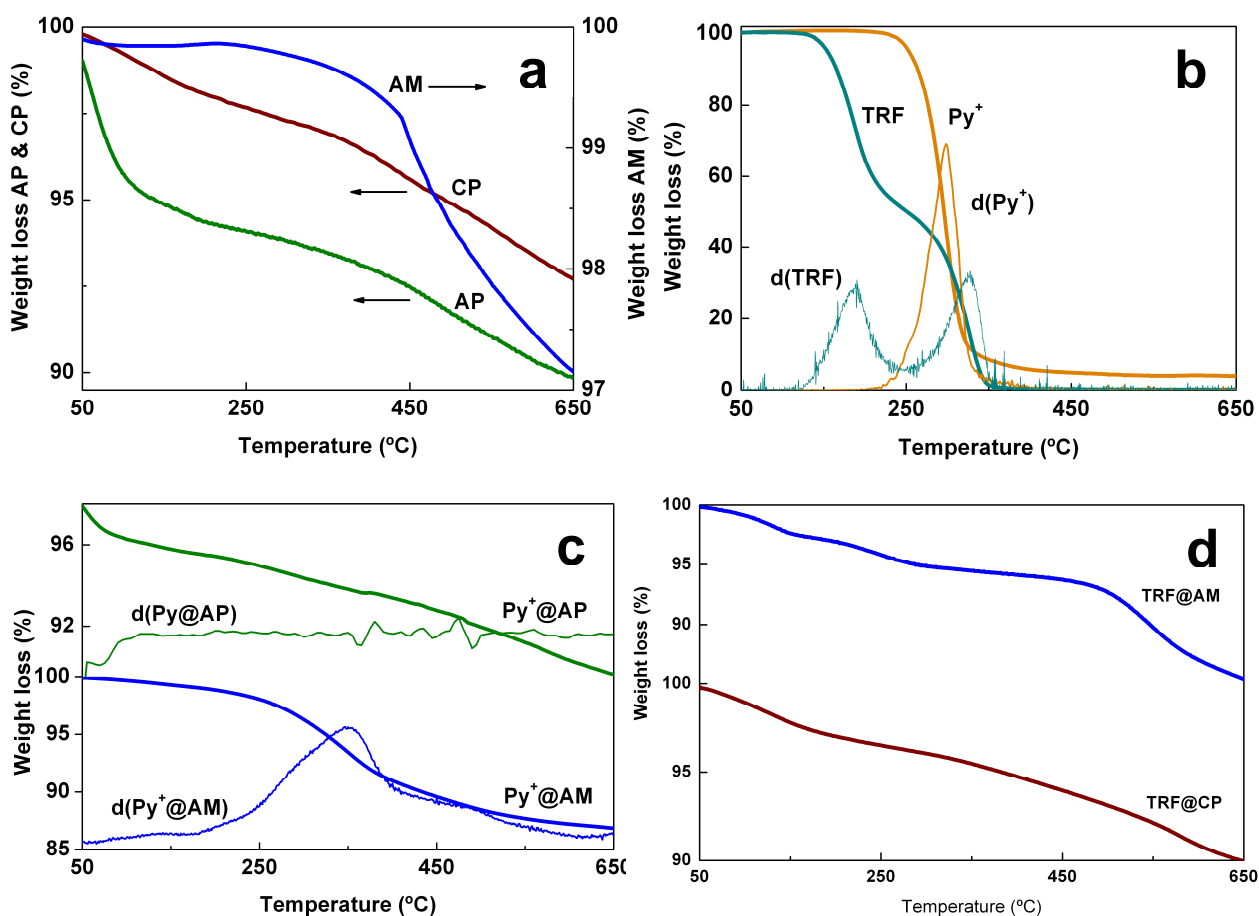
Figure 4. TGA curves of a) pristine matrices, b) commercial Py$^+$ cation and TRF antiaggregant, c) samples obtained after impregnation with pyrylium and d) with triflusal. Curves labeled as d(guest@matrix) are the derivatives of the respective TGA curves.

For the samples impregnated with the therapeutic agent, both the aerogel and composite NPs show a gentle slope before 150 ℃, which was attributed to the loss of water. From 150 ℃ to 500 ℃ degradation of the drug entrapped in AM occurs, while it decomposed in the range 160-380 ℃ when placed in the CP sample.

X-Ray diffraction

Powder X-ray diffraction and microdiffraction were performed on triflusal impregnated matrices to analyze the solid state of the drug in the matrix. Results are shown in Fig. 5a (triflusal encapsulated in the aerogel monolith) and Fig. 5b (triflusal entrapped in composite NPs). Neither the spectrum of aerogel nor the particles display peaks corresponding to TRF or HTB crystal. Concerning CP samples, it was observed the presence of the characteristics peaks for magnetite [15], more clearly visible in untreated $Fe_3O_4@SiO_2$ NPs.
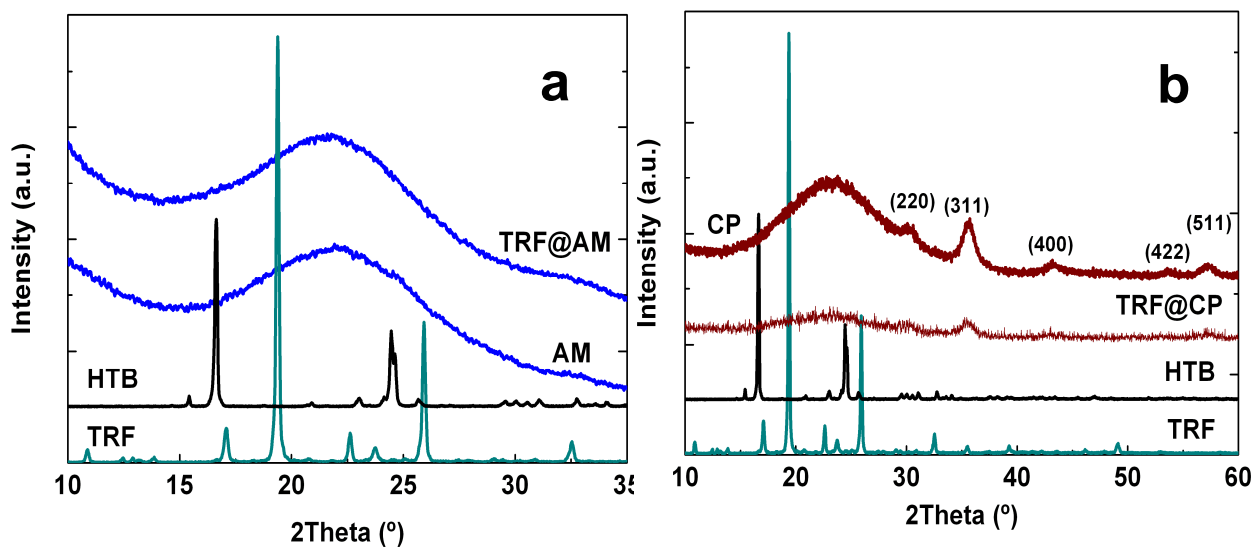
Figure 5. XRD spectra of: a) therapeutic agent TRF and methabolite HTB, pristine matrix AM and the corresponding impregnated sample TRF@AM, and b) TRF, HTB, pristine matrix CP and the respective impregnated material TRF@CP.

Leaching behavior of pyrylium impregnated compounds

The purpose of the leaching study was to elucidate the stability in water of the encapsulated cation, since the free cation is unstable in water at neutral pH. Prepared samples were submerged in distilled water during 12 days. It is important to remark that, after this relatively long period of time, the materials still maintained their characteristic yellow/orange color of the impregnated product, indicating that both leaching and degradation of the cation were minor. To monitor the leaching behavior of the different materials, aliquots of the liquid phase were withdrawn at given times and analyzed by UV-vis spectrophotometry. According to the literature, triphenylpyrylium salt organic solution has a broad band in the region 370–480 nm, [16, 17] while its precursor present appreciable absorption at wavelengths between 200 and 350 nm. (Following the designed leaching protocol, after 5 d in water, the spectra of the as-prepared $Py^+@AM$ sample (Fig. 6a) shows absorption between 225 and 325 nm. However, they did not show the presence of any significant amount of organic compounds in the refreshed water added afterwards and measured on day 12. A similar behavior was observed for $Py^+@AP$ material.

Since the desorption of the organic material only occurs in the first stage, the leaching should came from impregnated material located on the most external part of the matrix, where the cation is less stabilized than in the most internal pores. It has been previously reported that simple deposition of these cations on the external surface of silica does not prevent hydrolysis. [18] Considering that the UV-vis absorption at day 1 is much lower than at day 5, leaching behavior is probably controlled by diffusion through the nanopores. Thus, impregnated molecule in the studied matrices showed higher hydrolysis stability when encapsulated than as non-encapsulted in crystalline form.
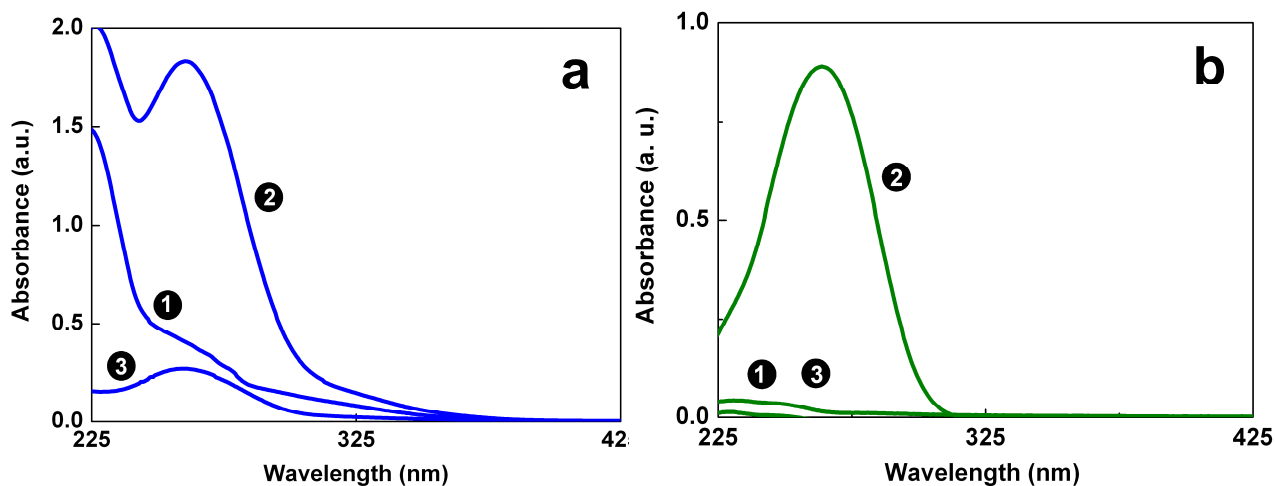
Figure 6. The leaching behavior in water of Ph_3Py^+ impregnated samples measured using UV-vis spectroscopy: a) AM and b) AP. The numeric notation indicates the timing of aliquot absorption measurements: ❶ after 1 d, ❷ after 5 d, and ❸ after 12 d.

Drug release monitoring

A chromatographic analysis was performed to characterize the drug delivery profile of TRF (HTB) impregnated materials. Fig. 7 shows the results obtained in 10 mM HCO_3^-/CO_3^{2-} solution. Two different release behaviors were observed for drug@AM and drug@CP samples.
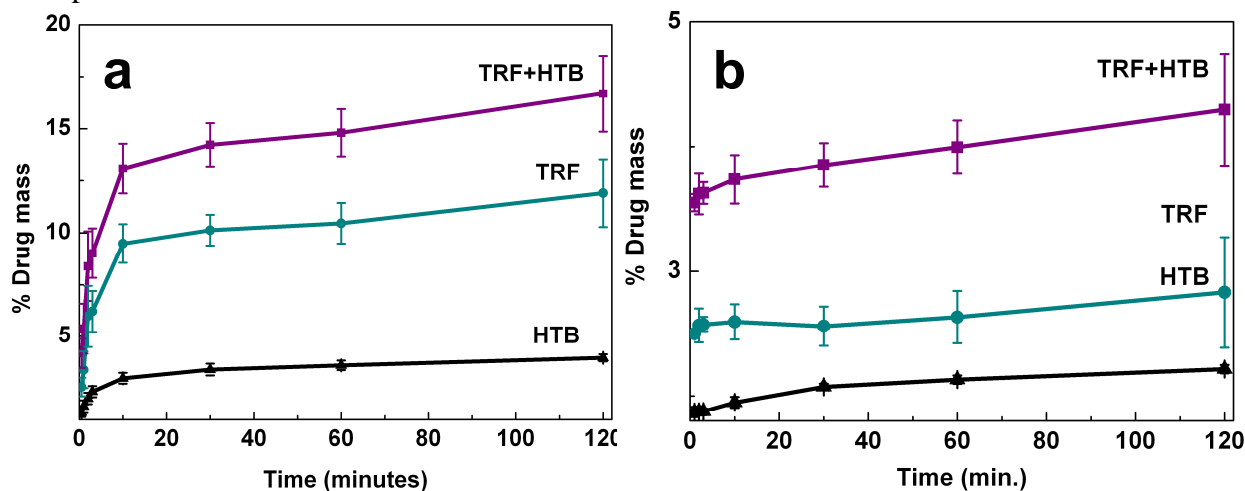

Figure 7. Drug release profiles obtained chromatographically for drug impregnating: a) AM, and b) CP systems in aqueous solution at pH 7.4.

The overall concentration of TRF and HTB delivered by AM samples increased progressively during the studied period with a final value after 2 h of 16.7 wt% of active compound released to the basic medium. On the other hand, a faster release was observed for composite NPs impregnated with the drug, since most of the drug was delivered in the first ten minutes. In this material, 4.1 wt% of the drug was dissolved from the nanoporous matrix after 2 h.

CONCLUSIONS

In particular, we have reported on hybrid inorganic-organic nanoestructured materials consisting of aerogels and aerogel inspired materials as suitable hosts to stabilize organic photoactive cations or to carry and enhance the bioavailability of a therapeutic agent.
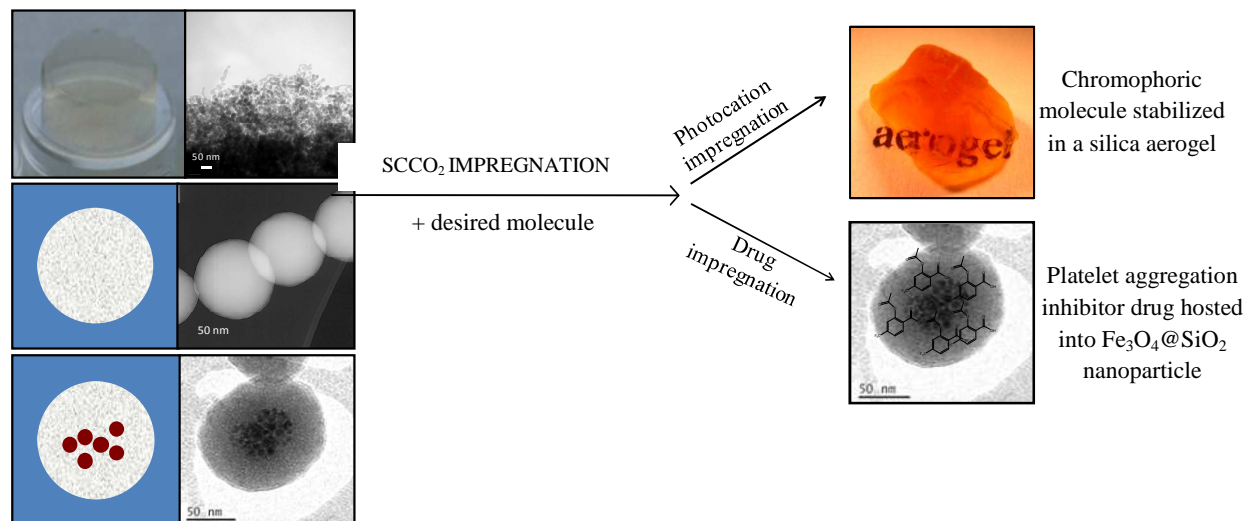
REFERENCES

[1] ROIG A., MATA I., MOLINS E., MIRAVITLLES C., TORRAS J., LLIBRE, J. J. Eur. Ceram. Soc., Vol. 18, **1998**, p. 1141.

[2] MONER-GIRONA M., ROIG A., MOLINS E., LLIBREJ., J. Sol-Gel Sci. Technol., Vol. 26, **2003**, p. 645.

[3] TABOADA E., SOLANAS E., RODRÍGUEZ E., WEISSLEDER E., ROIG A., Adv. Funct. Mater., Vol. 19, **2009**, p. 2319.

[4] MURILLO-CREMAES N., LÓPEZ-PERIAGO A., SAURINA J., ROIG A., DOMINGO C., Green. Chem., **2010**, Vol. 12, p. 2196.

[5] LÓPEZ-PERIAGO A.M., FRAILE J., GARCÍA-GONZÁLEZ C.A., DOMINGO C., J. Supercrit. Fluids, Vol. 50, **2009**, p. 305.

[6] LÓPEZ-PERIAGO A.M., VEGA A., SUBRA P., ARGUEMÍ A., SAURINA J., GARCÍA-GONZÁLEZ C.A., DOMINGO C., J. Mater. Sci., Vol. 43, **2008**, p. 1939.

[7] SANJUÁN A., AGUIRRE G., ALVARO M., GARCÍA H., Appl. Catal., B, Vol. 15, **1998**, p. 247.

[8] MIRANDA M.A., GARCIA H., Chem. Rev., Vol. 94, **1994**, p. 1063.

[9] RAMIS J., MIS R., J. Forn, Eur. J. Drug Metab. Pharmacokinet. Vol. 16, **1991**, p. 261.

[10] LÓPEZ-PERIAGO A.M., GARCÍA-GONZÁLEZ C.A., SAURINA J., DOMINGO C., Microporous Mesoporous Mater., Vol. 132, **2010**, p. 357.

[11]   ARGUEMÍ A., LÓPEZ-PERIAGO A.M., DOMINGO C., SAURINA J., J. Pharm. Biomed. Anal. Vol. 46, **2008**, p. 456.

[12] ANDANSON J.M., LÓPEZ-PERIAGO A.M., GARCÍA-GONZÁLEZ C.A., DOMINGO C., KAZARIAN S.G., Vib. Spectrosc., Vol. 46, **2009**, p. 183.

[13]   Infrared Spectra of Adsorbed Molecules, ed. L. H. Little, Willmer Brothers, Ltd. New York, 1996.

[14]   ARQUES A., AMATA A.M., SANTOS-JUANES L., VERCHER R.F., MARÍN M.L., MIRANDA M.A., J. Mol. Cat. A, **2007**, Vol. 271, p. 221.

[15] CORNELL R.M., SCHWERTMANN U., The iron oxides: structure, properties, reactions, occurrences and uses, W.   VCH, Editor. **2003**.

[16]   FAKIS M., TSIGARIDAS G., POLYZOS I., GIANNETAS V., PERSEPHONIS P., SPILIOPOULOS I., MIKROYANNIDIS J., Chem. Phys. Lett., Vol. 342, **2001**, p. 155.

[17]   DUXBURY D.F., Chem. Rev., Vol. 93, **1993**, p. 381.

[18]   MIRANDA M.A., AMAT A.M., ARQUES A., Catal. Today, Vol. 76, **2002**, p. 113.